

Sébastien Roger · Pierre Besson
Jean-Yves Le Guennec

Influence of the whole-cell patch-clamp configuration on electrophysiological properties of the voltage-dependent sodium current expressed in MDA-MB-231 breast cancer cells

Received: 31 July 2003 / Accepted: 11 September 2003 / Published online: 31 October 2003
© EBSA 2003

Abstract Voltage-gated ionic channels are known to be involved in oncogenesis. However, only a few studies describe the functional characteristics of these channels or the mechanisms by which they are involved in the proliferation and invasive processes. Breast cancer cells proliferate and migrate under the constant activation of growth factors, hormones, extracellular matrix interactions, etc. It would thus not be surprising if the activity of the ionic channels was modulated by intracellular regulation pathways such as kinases or phosphatases, which in turn can affect oncogenic properties. In the present study, we investigated some of the electrophysiological properties of the fast inward sodium current found in the breast cancer cell line MDA-MB-231 with two configurations of the patch-clamp technique. With perforated patch, a configuration which allows to keep the cytoplasm intact, the mean current amplitude was lower, the relative conductance–voltage relationship was shifted to more positive potentials and the recovery from inactivation was accelerated when compared to ruptured patch, where the cytoplasm is dialysed by the intrapipette solution. There was no difference in availability–voltage (pseudo-steady-state inactivation) relationship and in time to peak of the current. These results suggest that regulation mechanisms, possibly involving kinases or phosphatases, are switched off when the cytoplasm is diluted. We propose that such a regulation can modulate the functioning of the channels even in the absence of membrane voltage changes, which in turn can affect oncogenic properties. This finding is of importance when evaluating the physiopathological role of ionic channel in cancer development.

Keywords Amphotericin · Cancer · Perforated patch-clamp · Ruptured patch-clamp · Sodium channels

Abbreviations *DMEM* Dulbecco's modified Eagle's medium · *FBS* fetal bovine serum · *PP* perforated patch · *RP* ruptured patch

Introduction

The precise roles of ionic channels in carcinogenesis, tumour progression and in metastatic behaviour are poorly understood. Ionic channels are known to be important for many cellular functions and are involved in several diseases. Roles for ionic channels in cancer cells have been established in cell cycling (Wonderlin et al. 1995), apoptosis (Nagy et al. 1995), cell adhesion (Arcangeli et al. 1993), cell movement (Arcangeli et al. 1993; Grimes et al. 1995), exocytosis (Sheng et al. 1996), proliferation (Ouadid-Ahidouch et al. 2000, 2001; Woodfork et al. 1995) and multidrug resistance (Yamashita et al. 1987), all of which have direct relevance to the neoplastic process. Ionic channels are highly regulated by a wide range of hormones and factors acting through phosphorylation (Hille 1992). However, while hormones and growth factors play a role in carcinogenesis (see Strobl et al. 1995 for review), regulation of ionic channels has never been studied in cancer cell lines. Among women, breast cancer is the commonest cancer and the first cause of death. In breast cancer, the putative role of ionic channels has been known since the work of Marino et al. (1994). Since this pioneer work, the role of ionic channels in breast cancer cell lines has focused mainly on potassium channels (Strobl et al. 1995; Wonderlin et al. 1995; Woodfork et al. 1995; Ouadid-Ahidouch et al. 2000, 2001). Recently, we found a fast inward sodium current in a highly metastatic cell line, MDA-MB-231 (Roger et al. 2003). This current is involved in the invasion process through mechanisms which still have to be determined.

Presented at the Biophysical Society Meeting on 'Ion Channels—from structure to disease' held in May 2003, Rennes, France

S. Roger · P. Besson · J.-Y. Le Guennec (✉)
Nutrition, Croissance et Cancer, Emi-U 0211 Inserm, Faculté de
Médecine, 2 Bd Tonnellé, 37032 Tours, France
E-mail: leguennec@univ-tours.fr
Tel.: +33-2-47366130
Fax: +33-2-47366226

In this study, we compare the properties of the fast inward voltage-gated sodium current found in MDA-MB-231 cells studied with two configurations of the patch-clamp technique: ruptured patch versus perforated patch using amphotericin B. In electrophysiologically well-defined preparations such as cardiac cells, it has been shown that the configuration of the patch-clamp can alter the regulation of some ionic currents (Liu and Kennedy 1998; Calaghan et al. 2001). Thus, dialysis of the cytoplasm, occurring in the ruptured patch-clamp configuration, can modify the regulation by phosphorylation. By comparing the results obtained in both patch-clamp configurations, we discuss possible ways for the sodium current to be regulated and in turn to regulate cell invasion.

Methods

Cell culture

The breast cancer cell line MDA-MB-231 was purchased from the American Type Culture Collection (Rockville, Md., USA) at passage 28. All experiments were carried out within 20 additional passages. Cells were grown in Dulbecco's modified Eagle's medium (DMEM; 4.5 g/L glucose, 584 mg/L glutamine and 3.7 g/L NaHCO₃) supplemented with 5% fetal bovine serum (FBS) and with 1% antibiotics (mixture of 5000 U/mL penicillin and 5000 µg/mL streptomycin). Cells were grown in an atmosphere saturated with humidity at 37 °C and 5% CO₂.

Electrophysiology

For electrophysiological analysis, cells were seeded into 35-mm Petri dishes at 2500 cells/cm². Before patch-clamping, the growth medium was rinsed and replaced with a physiological saline solution (PSS, see Solutions). Patch pipettes were pulled from non-heparinized haematocrit tubes to a resistance of 3–5 MΩ. Currents were recorded under voltage-clamp mode at room temperature using an Axopatch200 B patch-clamp amplifier (Axon Instrument, Burlingame, Calif., USA). Analogue signals were filtered at 5 kHz, using a five-pole low-pass Bessel filter, and sampled at 10 kHz using a 1322A Digidata converter. PClamp software (v8.1, Axon Instrument) was used for generation of voltage commands, acquisition and analysis of the whole-cell current. Two configurations of the whole-cell patch-clamp technique were used: ruptured patch and perforated patch. In ruptured patch (RP) conditions, the patched membrane under the pipette was broken to electrically access the interior of the cell and dialyse it with the intrapipette solution (see Solutions). To keep the cytoplasm intact and to avoid the wash out of some intracellular regulators of ionic channels (Horn and Marty 1988; Calaghan et al. 2001), we used the perforated patch (PP) in other experiments. In this configuration, the pipettes were filled with the same intrapipette solution but containing 400 µg/mL amphotericin B. Cell capacitance and series resistances were electronically compensated by about 60%. The P/2 subpulse correction of cell leakage and capacitance was used. The cell under investigation was continuously superfused with physiological saline solution (flow rate 500 µL/min).

Inward currents were recorded by depolarizing the cells from a holding potential of –100 mV to a maximal test pulse of –5 mV (corresponding to the maximal inward current) for 30 ms every 500 ms. The protocol to build the current–voltage (*I*–*V*) curve was as follows: from a holding potential of –100 mV, the membrane was stepped to potentials between –80 to +55 mV, with 5-mV increments, for 50 ms at a frequency of 2 Hz. Availability curves were obtained by using the *I*–*V* curve procedure, as a prepulse,

immediately followed by a depolarizing pulse to –5 mV for 50 ms, as a test pulse. In this case, currents triggered by the test pulse were normalized to the amplitude of the current triggered from –100 mV.

Conductance (*g*) through Na⁺ channels was normalized (relative conductance, *g*) by dividing the peak Na⁺ current by the driving force (*E_m*–*E_{Na}*), where *E_{Na}* is the equilibrium potential for Na⁺ derived from the Nernst equation and *E_m* the applied voltage normalized to the maximal conductance. At voltages more positive than that giving the maximal conductance, relative conductance was set to 1. Relative conductance and availability data were fitted with a Boltzmann function of the form:

$$Y = \frac{1}{1 + \exp(V_{1/2} - V)^k} \quad (1)$$

where *Y* is the fitted parameter (conductance or availability), *V*_{1/2} is the voltage at which half-maximal conductance or availability occurs, *k* is the slope factor determining how steeply conductance or availability change with voltage and *V* is the command voltage.

To study the recovery from inactivation of the inward current, two 30 ms pulses (prepulse and test pulse) from the holding potential at –100 mV were separated by a variable 5–50 ms interpulse interval. The ratio of the current elicited by the test pulse to that elicited by the prepulse is plotted to give the reactivation curve of the current. Points were then fitted by a monoexponential function as follows to obtain the time constant of recovery from inactivation:

$$\frac{I_{tp}}{I_{pp}} = A \times \exp\left(\frac{-t}{\tau}\right) \quad (2)$$

where *I*_{tp} is the amplitude of the current elicited by the second pulse (test pulse), *I*_{pp} is the amplitude of the current elicited by the first pulse (prepulse), *A* is the amplitude of the exponential, *t* is the time interval between the two pulses and *τ* is the time constant of reactivation. The *I*_{Na} amplitude was determined as the difference between the maximum peak inward current and the current amplitude at the end of the depolarizing pulse. Current amplitudes were normalized on cell capacitance to take into account differences in cell size and expressed as current density (pA/pF).

Solutions

The physiological saline solution (PSS) has the following composition (in mM): NaCl 140, KCl 4, MgCl₂ 1, CaCl₂ 2, D-glucose 11.1 and HEPES 10, adjusted to pH 7.4 with 1 M NaOH. The intrapipette solution has the following composition (in mM): K-aspartate 110, KCl 10, NaCl 10, MgCl₂ 8, K₂-ATP 8, EGTA 10, HEPES 10, adjusted to pH 7.1 with 1 M KOH. For PP, 400 µg/mL amphotericin was added to this solution.

All chemicals were purchased from Sigma-Aldrich (St Quentin, France).

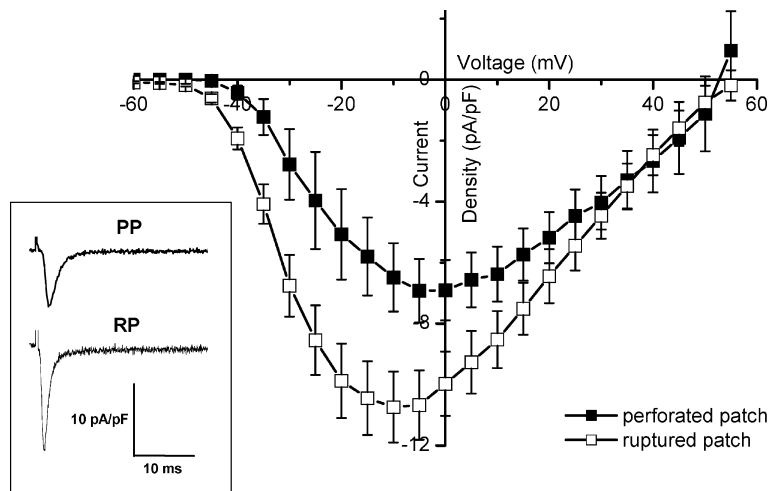
Statistics

Data are described as mean ± standard error of the mean (*n* = number of cells). Two-way repeated measures ANOVA followed by a Student–Newmann–Keuls test were used. *P* < 0.05 was considered as significant.

Results

Whatever the patch-clamp configuration used, when the membrane holding potential was set to –100 mV and the membrane depolarized to –5 mV for 30 ms, a rapid inward current was triggered which has been shown previously to be a TTX-resistant sodium current, i.e. which

Fig. 1 Influence of the patch configuration on $I_{\text{Na}}-V$ relationships. Mean current–voltage relationships were obtained from 26 cells in RP and 19 cells in PP. Empty squares and filled squares represent data obtained in RP and PP, respectively. Currents measured between -45 and $+10$ mV are significantly smaller in PP. The inset on the left shows an example of currents recorded from representative cells depolarized at -10 mV from a holding potential of -100 mV in PP (upper curve) and in RP (lower curve) (currents recorded from representative cells depolarized at -10 mV from a holding potential of -100 mV in PP (upper curve) and in RP (lower curve))



is blocked by micromolar concentrations of TTX (Roger et al. 2003). In order to characterize the current electrophysiologically, we built $I_{\text{Na}}-V$ curves in both RP and PP configurations (Fig. 1). In PP, the voltage threshold of the current and the maximum current amplitude are shifted rightward as compared to the current obtained with RP. Another difference is the amplitude of the current, which is significantly smaller at voltages ranging from -45 to $+10$ mV when measured with PP. At voltages between $+15$ and $+60$ mV, there is no significant difference in current amplitude in both configurations.

The decrease of current amplitude is associated with a significant rightward shift of the conductance–voltage curve (Fig. 2A), while a non significant rightward shift of the availability (pseudo-steady-state inactivation) curve was observed (Fig. 2B). Such results strongly suggest that the rightward shift of the $I_{\text{Na}}-V$ curve in PP is not due to screening of charge surfaces or different junction potentials but might be consecutive to the wash-out of some intracellular channel regulator in RP. To confirm this hypothesis, we measured the time constant of inactivation of the current, τ , at all voltages and the time to peak (TTP) of the current at -5 mV. Figure 3A shows that the time constant of inactivation depends on voltage but not on the patch configuration except at -30 mV, where a drop of the time constant is observed in PP but not in RP. This drop has been observed in all studied cells. Figure 3B confirms that lack of difference on the TTP measured at -5 mV.

Figure 4 shows the recovery from inactivation of I_{Na} in PP and in RP. With the PP configuration, recovery from inactivation is significantly faster than with RP ($P < 0.05$).

Discussion

Ionic currents are often studied in the RP configuration. In this configuration, replacement to a large extent of the cytoplasm with the solution inside the patch pipette

allows control of the intracellular ionic composition. However, the drawback is that the loss of intracellular regulators can interfere with the regulation of the

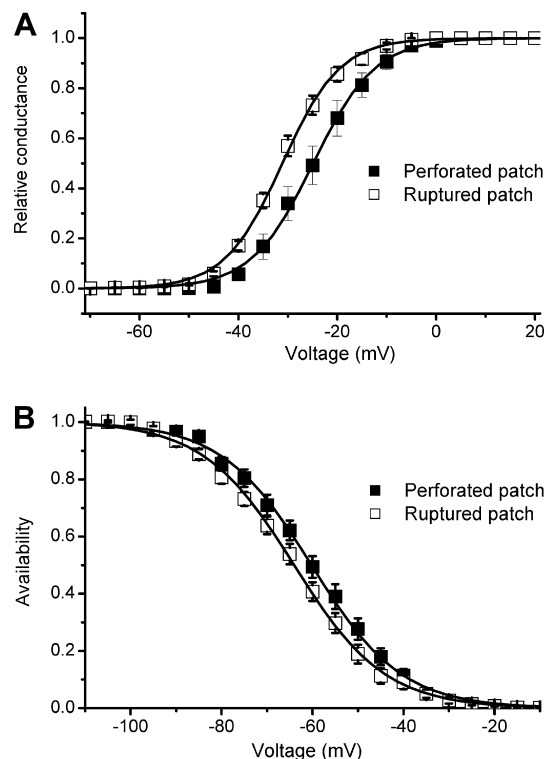


Fig. 2A, B Comparison of relative conductance–voltage and availability–voltage relationships in PP and in RP. Curves are fitted using a Boltzmann function (see Methods). Empty squares and filled squares represent data obtained in RP and PP, respectively. **A** The conductance–voltage relationship is significantly rightward-shifted in PP as compared to RP conditions. The half-conductance voltages calculated from the Boltzmann fits were -24.9 ± 0.2 mV ($n = 19$, PP) and -31.1 ± 0.1 mV ($n = 26$, RP). **B** The availability–voltage (pseudo-steady-state inactivation) relationships were not significantly different in the two configurations of the patch-clamp. The half-inactivation voltages calculated from the Boltzmann fits were -60.2 ± 0.3 mV ($n = 19$, PP) and -64.1 ± 0.2 mV ($n = 26$, RP)

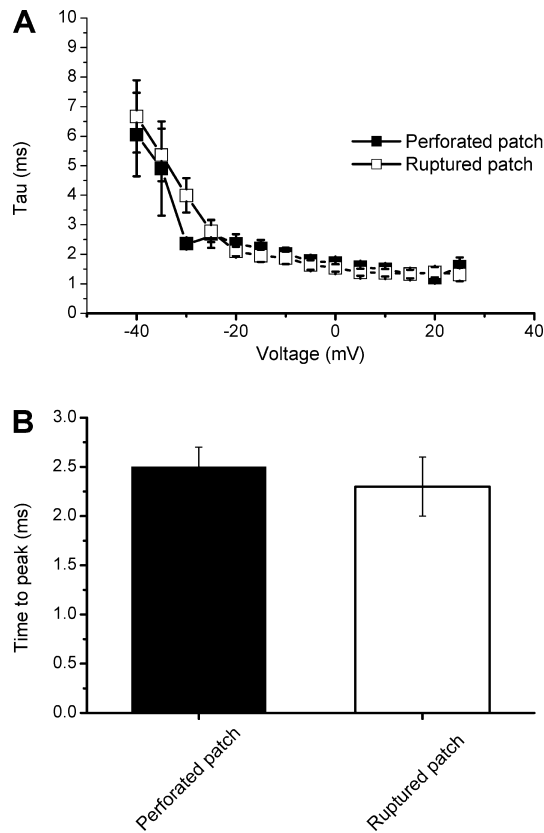


Fig. 3A, B Comparison of time constants of inactivation and time to peak of the current in PP and in RP. **A** Time constant of inactivation of the current, τ , was estimated using a monoexponential function. Empty squares and filled squares represent data obtained in RP ($n=26$ cells) and PP ($n=19$ cells), respectively. No significant difference is found except at -30 mV. **B** Mean time to peak of the current elicited at -5 mV from a holding potential of -100 mV in PP (filled bar, $n=19$ cells) and in RP (empty bar, $n=26$ cells). No significant difference is found

channel (Liu and Kennedy 1998; Calaghan et al. 2001). Cancer cells are constantly stimulated by environmental factors, growth factors, hormones, etc. These modulators can affect the membrane potential and in turn the activity of voltage-dependent ionic channels. Also, these agonists can activate kinases which in turn phosphorylate proteins such as ionic channels. Voltage-dependent sodium channels are regulated by intracellular kinases like PKC and PKA (Qu et al. 1994; Murphy et al. 1996). Such phosphorylations lead to changes in electrophysiological properties of the currents. In the present study, we found that I_{Na} electrophysiological features are different when measured with RP or PP. These differences cannot be attributed to different screening of surface charges or junction potential. Indeed, neither the reversal potential is significantly affected by the patch configuration nor the time constant of inactivation and the time to peak of the current. Also, the relative conductance–voltage relationship is significantly shifted to more positive potentials while the availability–voltage relationship is not.

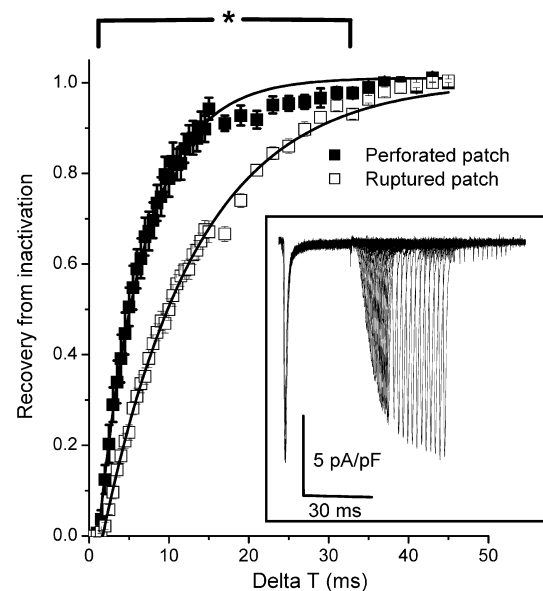


Fig. 4 Influence of the patch configuration on recovery from inactivation. Recovery from inactivation was obtained using the double-pulse protocol described in the Methods section. Curves are fitted with a monoexponential function (see Methods). Empty squares and filled squares represent data obtained in RP ($n=21$ cells) and PP ($n=16$ cells), respectively. Recovery from inactivation is significantly faster in PP than in RP conditions ($P<0.05$; the asterisk indicates time points which are significantly different). The mean time constants of reactivation calculated from the monoexponential fits of the experimental data were 6.0 ± 0.1 ms in PP and 11.8 ± 0.2 ms in RP. The inset shows an example of currents obtained during the double-pulse protocol with RP

The most likely explanation is that some intracellular regulators are lost after breaking the patch. In other preparations, such as cardiac cells, it has been shown that an intact cytoplasm was necessary for the α -1 adrenergic stimulation pathway to be effective (Liu and Kennedy 1998). It has also been shown that, without beta agonist and after microtubule disruption by colchicine, activation of the beta adrenergic stimulation pathway was detected with RP and not with PP (Calaghan et al. 2001). Possible explanations for the changes in the electrophysiological properties of the sodium channels in our conditions could be the loss of basal activation of kinases such as PKC and PKA after breaking the patch, or, on the contrary, that the dilution of the cytoplasm would lead to the activation of some kinases. To us, the most likely explanation is that, with an intact cytoplasm, there is a basal activation of kinases because cells are grown in a medium containing growth factors and hormones. It has been shown that PKC-dependent phosphorylation of sodium channels from neonatal rat heart cells induces a rightward shift of the availability curve and an acceleration of the recovery from inactivation (Watson and Gold 1997). The same modifications were observed in our experiments. However, in our study, the amplitude of the current is also affected and the relative conductance–voltage relationship is shifted. Thus, it is likely that other regulation pathways are involved.

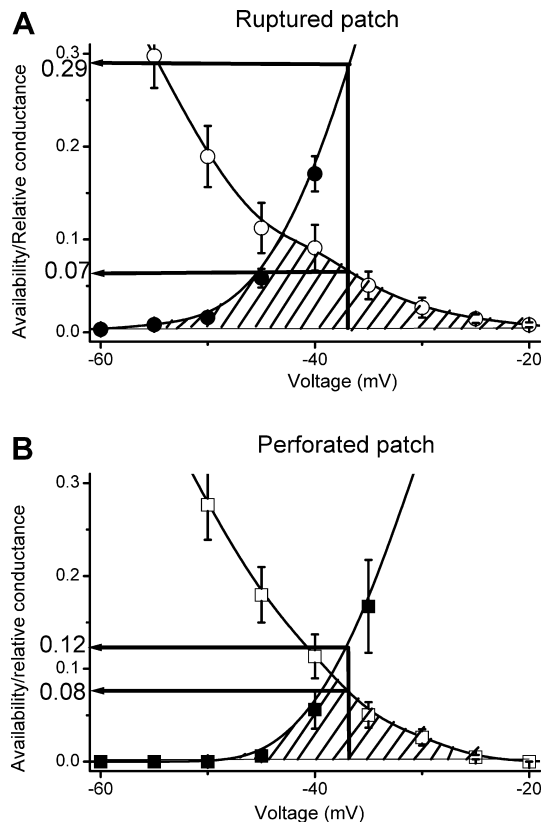


Fig. 5 Comparison of the window currents obtained in RP (A) and in PP (B). The *hatched areas* indicate the window of voltage at which a continuous entry of sodium occurs owing to an incomplete inactivation of the current. Relative conductance (*closed symbols*) and availability (*open symbols*) are indicated with the *arrows* at -37 mV, which approximately corresponds to the mean membrane potential measured in MDA-MB-231 cells

We previously showed that I_{Na} is involved in the invasivity of the MDA-MB-231 through an extracellular matrix-mimicking substrate (Matrigel) (Roger et al. 2003). We suggested that the involvement of the channel is linked to the presence of a window current at the resting membrane potential of these cells, which are not excitable. In the view of the present results, we propose that the current can modulate the invasivity of MDA-MB-231 cells through changes of the window current amplitude; thus the intracellular sodium homeostasis. As shown in Fig. 5, the window currents are different whether the current is studied in RP (Fig. 5A) or in PP (Fig. 5B). At a potential corresponding approximately to the mean membrane potential measured in our conditions (-36.8 ± 1.5 mV, $n=79$ cells in RP and -36.7 ± 2.4 mV, $n=26$ cells in PP), -37 mV, the calculated conductance (relative conductance \times availability) is decreased about two-fold in PP as compared to RP conditions. This means that the entry of sodium through the window current at this membrane potential is about two-fold larger in RP than in PP. These differences are only due to shifts in conductance- and availability-voltage relationships.

Thus, even without changes in the membrane voltage of non-excitable cells, the entry of sodium into the cell can be modulated.

References

- Arcangeli A, Becchetti A, Manini A, Mugnai G, De Filippi P, Tarone G, Del Bene M, Barletta E, Wanke E, Olivetto M (1993) Integrin-mediated neurite outgrowth in neuroblastoma cells depends on the activation of potassium channels. *J Cell Biol* 122:1131–1143
- Calaghan S, Le Guennec J-Y, White E (2001) Modulation of Ca^{2+} signalling by microtubule disruption in rat ventricular myocytes and its dependence on the ruptured patch-clamp configuration. *Circ Res* 88:e32–e37
- Grimes J, Fraser S, Stephens G, Downing J, Laniado M, Foster C, Abel P, Djamgoz M (1995) Differential expression of voltage-activated Na^{+} currents in two prostatic tumour cell lines: contribution to invasiveness in vitro. *FEBS Lett* 369:290–294
- Hille B (1992) Ionic channels of excitable membranes, 2nd edn. Sinauer, Sunderland, Mass., USA
- Horn R, Marty A (1988) Muscarinic activation of ionic currents by a new whole-cell recording method. *J Gen Physiol* 92:145–159
- Liu S, Kennedy R (1998) $\alpha 1$ -adrenergic activation of L-type Ca^{2+} current in rat ventricular myocytes: perforated patch-clamp recordings. *Am J Physiol* 274:H2203–H2207
- Marino A, Iliev I, Schwalke M, Gonzalez E, Marler K, Flanagan C (1994) Association between cell membrane potential and breast cancer. *Tumour Biol* 15:82–89
- Murphy BJ, Rogers J, Perdichizzi AP, Colvin AA, Catterall WA (1996) cAMP dependent phosphorylation of two sites in the alpha subunit of the cardiac sodium channel. *J Biol Chem* 271:28837–28843
- Nagy P, Panyi G, Jenei A, Bene L, Gaspar R, Matko J, Damjanovich S (1995) Ion channel activities regulate transmembrane signalling in thymocyte apoptosis and T-cell activation. *Immunol Lett* 44:91–95
- Ouadid-Ahidouch H, Chaussade F, Roudbaraki M, Slomianny C, Dewailly E, Delcourt P, Prevarskaya N (2000) Kv1.1 K^{+} channels identification in human breast carcinoma cells: involvement in cell proliferation. *Biochem Biophys Res Commun* 278:272–277
- Ouadid-Ahidouch H, Le Bourhis X, Roudbaraki M, Toillon R, Delcourt P, Prevarskaya N (2001) Changes in the K^{+} current-density of MCF7 cell during progression through the cell cycle: possible involvement of a h-ether-a-gogo K^{+} channel. *Rec Channels* 7:345–356
- Qu Y, Rogers J, Tanada T, Scheuer T, Catterall W (1994) Modulation of cardiac Na^{+} channels expressed in a mammalian cell line and in ventricular myocytes by protein kinase C. *Proc Natl Acad Sci USA* 91:3289–3293
- Roger S, Besson P, Le Guennec JY (2003) Involvement of a novel fast inward sodium current in the invasion capacity of a breast cancer cell line. *Biochim Biophys Acta* 1616:107–111
- Sheng Z, Rettig J, Cook T, Catterall W (1996) Calcium-dependent interaction of N-type calcium channels with the synaptic core complex. *Nature* 379:451–454
- Strobl J, Wonderlin W, Flynn D (1995) Mitogenic signal transduction in human breast cancer cells. *Gen Pharmacol* 26:1643–1649
- Watson LW, Gold MR (1997) Modulation of Na^{+} current inactivation by stimulation of protein kinase C in cardiac cells. *Circ Res* 81:380–386
- Wonderlin W, Wodfork K, Strobl J (1995) Changes in membrane potential during the progression of MCF-7 human mammary tumour cells through the cell cycle. *J Cell Physiol* 165:177–185

- Woodfork K, Wonderlin W, Peterson V, Strobl J (1995) Inhibition of ATP-sensitive potassium channels causes reversible cell-cycle arrest of human breast cancer cells in tissue culture. *J Cell Physiol* 162:163–171
- Yamashita N, Hamada H, Tsuruo T, Ogata E (1987) Enhancement of voltage-gated Na^+ channel current associated with multi-drug resistance in human leukemia cells. *Cancer Res* 47:3736–3741